Biochimica et Biophysica Acta 1863 (2016) 56–63

Contents lists available at ScienceDirect

Biochimica et Biophysica Acta

journal homepage: www.elsevier.com/locate/bbamcr

Functional hyperspectral imaging captures subtle details of cell metabolism in olfactory neurosphere cells, disease-specific models of neurodegenerative disorders

Martin E. Gosnell [a,c], Ayad G. Anwer [a], Juan C. Cassano [b], Carolyn M. Sue [b], Ewa M. Goldys [a,*]

[a] ARC Centre of Excellence for Nanoscale BioPhotonics, Macquarie University, Sydney 2109, New South Wales, Australia
[b] Department of Neurogenetics, Kolling Institute, Royal North Shore Hospital, Northern Clinical School, University of Sydney, New South Wales, Australia
[c] Quantitative Pty Ltd, ABN 17 165 684 186, Australia

ARTICLE INFO

Article history:
Received 24 June 2015
Received in revised form 17 August 2015
Accepted 25 September 2015
Available online 26 October 2015

Keywords:
Molecular analysis
Neurodegenerative disorders
MELAS
Metabolic imaging
Hyperspectral

ABSTRACT

Hyperspectral imaging uses spectral and spatial image information for target detection and classification. In this work hyperspectral autofluorescence imaging was applied to patient olfactory neurosphere-derived cells, a cell model of a human metabolic disease MELAS (mitochondrial myopathy, encephalomyopathy, lactic acidosis, stroke-like syndrome). By using an endogenous source of contrast subtle metabolic variations have been detected between living cells in their full morphological context which made it possible to distinguish healthy from diseased cells before and after therapy. Cellular maps of native fluorophores, flavins, bound and free NADH and retinoids unveiled subtle metabolic signatures and helped uncover significant cell subpopulations, in particular a subpopulation with compromised mitochondrial function. Taken together, our results demonstrate that multispectral spectral imaging provides a new non-invasive method to investigate neurodegenerative and other disease models, and it paves the way for novel cellular characterisation in health, disease and during treatment, with proper account of intrinsic cellular heterogeneity.

1. Introduction

Olfactory neurosphere (ONS) cells are easily accessible, patient-derived models of neurological disease [1]. They are harvested from the human olfactory mucosa, the organ of smell in the nose, which regenerates throughout life. This neural tissue is accessible in human adults and it demonstrates disease-dependent cell biology alterations in Alzheimer's and Parkinson's diseases, Rett syndrome, fragile X syndrome, schizophrenia, MELAS and other diseases [2–8]. The analysis of such cells provides new routes for the understanding of the pathogenesis of complex neurodegenerative conditions. Relative to other tissue neurons exhibit intense metabolic demands, therefore impairment of cellular metabolism accompanies many neurodegenerative diseases. Thus new methods are required to characterise and quantify metabolism of neural and other cells and tissue on a single cell level. Such methods are important for accurate early diagnosis, treatment monitoring and the development of therapies.

Imaging of endogenous cell fluorophores including nicotinamide adenine dinucleotide (NADH), nicotinamide adenine dinucleotide phosphate (NADPH), flavin adenine dinucleotide (FAD) and flavin mononucleotide (FMN) to investigate cell metabolism has been pioneered by Chance et al.[9]. By using optical microscopy techniques, these autofluorescent compounds can be easily observed providing insights into metabolic activity in cells without altering them with exogenous labels [10–27]. Multiphoton and fluorescence lifetime imaging microscopy (FLIM) have been the leading methods of cellular autofluorescence imaging with pioneering works by Skala et al. [10–12], Gratton et al.[15–20], and others. Multiphoton and FLIM imaging make it possible to determine the relative amounts of FAD and reduced NADH and to distinguish their free and protein-bound forms. This has been used to document increased glycolysis in cancer cells [10–12]. Although quantitative analysis of autofluorescence has been previously explored in multiphoton and FLIM modalities, there has been no previous in-depth work concerned with single photon excited fluorescence. This simple approach provides clinically relevant information, and it can be carried out by using unsophisticated, low cost instrumentation.

Here we report the application of hyperspectral autofluorescence analysis to functional, metabolic imaging of patient-derived ONS

* Corresponding author.
E-mail address: ewa.goldys@mq.edu.au (E.M. Goldys).
URL: http://www.quantitative.net.au (M.E. Gosnell).

http://dx.doi.org/10.1016/j.bbamcr.2015.09.030

cells suffering from the mitochondriopathy MELAS. MELAS syndrome is commonly attributed to the m.3243A > G mitochondrial DNA (mtDNA) point mutation within the *MT-TL1* gene [28–31]. This mutation is thought to disrupt respiratory chain complex assembly as reflected by impaired mitochondrial protein synthesis [28] and reduced mitochondrial respiratory chain enzyme activities [29]. Mitochondrial dysfunction follows, with studies reporting reduced mitochondrial membrane potential, with a parallel increase in reactive oxygen species production leading to reduced ATP production [32] and induction of mitochondrial permeability [29]. Cellular damage is apparent too, with increased glycolytic rate, impaired NADH response, decreased glucose oxidation and increased lactate production [31]. This defective oxidative metabolic state is thought to influence the clinical expression of disease. Because highly metabolic cells such as myocytes and neurons are highly dependent on efficient mitochondrial function, the percentage of mutant mtDNA relative to wild-type mtDNA known as the "mutational load" is important for determining whether the cell will be affected by the mutation or not. This poorly understood phenomenon known as heteroplasmy, the existence of both wild-type and mutant mtDNA within a cell or tissue is unique to mitochondriopathies. Earlier studies have demonstrated that high mutational load is detrimental to metabolism. Thus the analysis method that is able to yield quantitative insights concerning metabolism of individual live cells as well as their populations is a valuable tool to improve the understanding of this and other mitochondrial diseases. This work demonstrates that a simple hyperspectral imaging system coupled to a conventional wide-field microscope and high content analysis of the images provides novel insights into cell metabolic signatures, their heterogeneity and MELAS disease biology.

This study examines the effect of MELAS mutational load and the shift in heteroplasmy due to galactose treatment on cell metabolism. To this aim we have cultured ONS cells from both control and MELAS patients with greatly varying low (11%) and high (44%) mutational loads. We have subsequently exposed them to galactose-supplemented medium which has been shown to cause a reduction in mutational load [33,34]. The cells were imaged to observe their autofluorescence characteristics. Throughout this work, hyperspectral autofluorescence images of live cells have been obtained at a number of excitation wavelength ranges between 334 and 495 nm (each approximately 10 nm wide). The emission is detected in the range 570 nm–605 nm. More details are described in the Methods section and in Supplementary Material S1–S5.

2. Results

2.1. Hyperspectral imaging can distinguish MELAS patients from healthy controls and sheds light on the effectiveness of galactose treatment

We present the results of hyperspectral autofluorescence characterisation of the ONS cells with low (11%) and high (44%) mutational loads of the m.3243A > G MELAS mutation ("MELAS ONS cells") and corresponding control cells (control 1 for 11% and control 2 for 44% MELAS mutational load, respectively). Hyperspectral data correlations have been removed by using PCA as described in Supplementary Material Section S4. Subsequently, average cell spectra (represented here by single data points) have been plotted in a two-dimensional spectral space produced by the linear discriminant analysis (LDA, see Supplementary Material S4). These are presented in Fig. 1 a where the axes represent the directions onto which the cellular data have been projected by LDA. The LDA optimally separates the three groups of cells: healthy cells from both controls 1 and 2, 11% mutant MELAS and 44% mutant MELAS cells.

Clear separation of clusters observed in Fig. 1 a indicates that the cells from MELAS patients can be distinguished from control cells. Moreover, the cells from two different MELAS patients also form different clusters, thus all three cell classes are well separated. To statistically analyse the cluster separations, a second LDA projection of cell data was carried out [35]. For this new projection, two classes of cells were chosen at a time, and their average spectra were projected onto a common line. This approach visualises cell distributions by histograms (Fig. 1 b–g). We found that every pair of classes selected among control, MELAS, MELAS galactose treated cell classes gave p-values in the Kolmogorov–Smirnov test of less than 10^{-12}, consistently with Fig. 1 a [36,37]. The Kolmogorov–Smirnov test if passed with $p < 0.05$ allows us to reject the null hypothesis that the samples are drawn from the same distribution.

The multispectral autofluorescence analysis of cells that have undergone galactose treatment to reduce mutational load is shown in Fig. 1 a. In this figure, the clusters of MELAS treated cells are located between the control population and the MELAS population. The histograms produced by pairwise LDA projections are significantly different as shown in Fig. 1 d–g. Thus multispectral imaging makes it possible to distinguish MELAS ONS cells from control cells and also quantifies the response of such cells to pharmacological interventions.

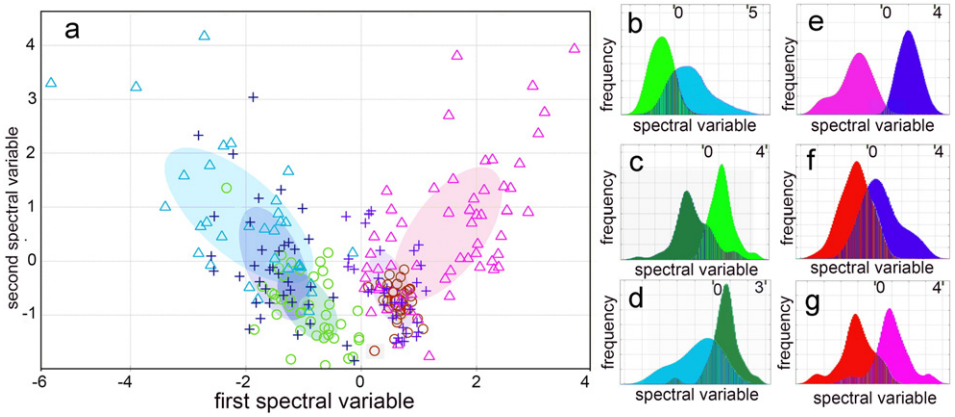

Fig. 1. Spectral projections of autofluorescent properties of ONS cells. Controls 1 and 2, 11% MELAS and 44% MELAS as well as 11% MELAS galactose treated and 44% MELAS galactose treated cells form statistically separate clusters with respect to autofluorescence properties. **a**) Scatter plot of average cell spectra in optimised spectral space. Small markers represent average cell spectra for each cell; the colour of these small markers identifies cell populations from different patients. Green circles: control1 cells (for 11% MELAS); red circles: (control 2 for 44% MELAS); cyan triangles: 11% MELAS; dark green crosses: 11% MELAS galactose treated; pink triangles: 44% MELAS; blue crosses: 44% MELAS galactose treated cells. Ovals — regions within the single standard deviation from the mean values for each cell population; (**b**–**g**) histograms (Parzen estimates, see Supplementary Material S4) of the selected pairs of cell classes. Numbers in brackets give statistical distance; p-values for class separation are less than 10^{-12}; **b**) 11% MELAS — cyan, control 1 — green (1.87); **c**) 11% MELAS galactose treated— dark green, control 1 — green (1.97); **d**) 11% MELAS — cyan, 11% MELAS galactose treated — dark green (1.15); **e**) 44% MELAS — pink, 44% MELAS galactose treated — blue (8.33); **f**) 44% MELAS galactose treated — blue, control 2 — red (1.23); **g**) 44% MELAS — pink, control 2 — red (2.08). Spectral variables are distance measures along the directions onto which the cell data have been projected (see Supplementary Section S4.1).